PPPL-2058

UC20-A,D,G

I-12390

PPPL-2058
Dr. 1966-6

PPPL--2058

DE84 003464

EFFECTS OF ION CYCLOTRON HARMONIC DAMPING ON CURRENT DRIVE IN THE LOWER HYBRID FREQUENCY RANGE

By

K.L. Wong and M. Ono

NOVEMBER 1983

PLASMA PHYSICS LABORATORY

PRINCETON UNIVERSITY
PRINCETON, NEW JERSEY

PREPARED FOR THE U.S. DEPARTMENT OF ENERGY,
UNDER CONTRACT DE-AC02-76-CHO-3073.

EFFECTS OF ION CYCLOTRON HARMONIC DAMPING ON CURRENT DRIVE IN THE LOWER HYBRID FREQUENCY RANGE

K.L. Wong and M. Ono

Plasma Physics Laboratory

Princeton University, Princeton, New Jersey 08544

ABSTRACT

We investigate the ion cyclotron harmonic damping effects on slow and fast waves in the lower hybrid frequency range for tokamak reactor parameters. Inclusion of the higher order terms in the hot plasma dielectric tensor introduces ion cyclotron harmonic damping; these terms also contribute to the real part of the dispersion relation and affect the wave trajectories. However, wave absorption by 15 keV deuterium and tritium ions can be avoided by choosing the slow wave frequency above the lower hybrid frequency and the fast wave frequency below the lower hybrid frequency. But preliminary estimates show that energetic alpha particles tend to absorb both the slow and the fast waves. This absorption may become a serious obstacle for fusion-reactor current drive in the lower hybrid frequency range.

I. INTRODUCTION

The research effort in lower hybrid waves has, in recent years, shifted from ion heating to current drive[1] due to the strong interest in steady-state tokamaks. Recent impressive success in lower hybrid wave (slow wave) current-drive experiments[2-8] makes it worthwhile to investigate the detailed wave properties in reactor parameters. Under ideal situations, the theoretical current drive efficiency via electron Landau damping (ELD) is only marginally acceptable for reactor applications.[9] Therefore, it is important to investigate whether or not there are other undesirable mechanisms that can further reduce the current drive efficiency. One obvious mechanism is ion cyclotron harmonic damping (ICHD) on the waves. For typical tokamak parameters, the lower hybrid frequency is much higher than the ion cyclotron frequency ($\omega/\omega_{ci} \sim 50$) so that ion heating is possible only if $k_\perp \rho_i$ is large enough. $k_\perp$ denotes the wave number perpendicular to the magnetic field, ρ_i denotes the ion Larmor radius, ω and ω_{ci} denote the wave frequency and the ion cyclotron frequency, respectively. Large values of $k_\perp \rho_i$ are known to occur near the lower hybrid resonance and it is precisely upon this phenomenon [10] that earlier lower hybrid wave <u>heating</u> experiments were based. In this paper we investigate the effect of this same mechanism on lower-hybrid <u>current drive</u>. In order to calculate accurately the effect of large $k_\perp \rho_i$ on the fast or slow wave dispersion relation, one has to keep many terms in the hot plasma dielectric tensor. In Sec. II of this paper, we present analytic and numerical linear damping calculations in a Maxwellian plasma. Both wave polarizations (slow and fast waves) in the lower hybrid frequency range are considered. In Sec. III, we estimate the wave absorption by α-particles which have a non-Maxwellian distribution function. The major findings from this analysis are: (a) the high order terms in the hot plasma dielectric tensor

can be important, (b) ICHD by 15 keV ions can be avoided by proper choice of wave frequency, and (c) wave absorption by energetic alpha particles appears to be a serious problem for both the slow and the fast waves in the lower hybrid frequency range.

II. ICHD BY MAXWELLIAN IONS

Within the range of validity of the WKB approximation, the wave equation in a plasma is obtained as $\vec{n} \times (\vec{n} \times \vec{E}) + \overleftrightarrow{K} \cdot \vec{E} = 0$ where $\vec{n} = \vec{k}\, c/\omega$ is the vector index of reflection and $\overleftrightarrow{K}$ is the hot plasma dielectric tensor. The determinant associated with the wave equation gives the local wave dispersion relation $D(\omega, \vec{k}) = 0$. In order to calculate the spatial damping rate for a weakly damped wave propagating across the magnetic field, we constrain ω and $k_\parallel$ as real quantities while $\vec{k}_\perp = \mathrm{Re}\,(\vec{k}_\perp) + i\,\mathrm{Im}\,(\vec{k}_\perp)$ is complex; the subscripts "$\parallel$" and "$\perp$" denote the components parallel and perpendicular to the external magnetic field. From perturbation analysis, one can easily obtain

$$\mathrm{Re}\,\{D(\omega,\ \mathrm{Re}\,(\vec{k}_\perp),\ k_\parallel)\} = 0\ , \tag{1a}$$

$$\mathrm{Im}\,(\vec{k}_\perp) = -\left.\frac{\mathrm{Im}\,\{D(\omega,\ \vec{k}_\perp,\ k_\parallel)\}}{\dfrac{\partial}{\partial \vec{k}_\perp}\{\mathrm{Re}\,[D(\omega,\ \vec{k}_\perp,\ k_\parallel)]\}}\right|_{\vec{k}_\perp\ =\ \mathrm{Re}\,(\vec{k}_\perp)}\ . \tag{1b}$$

"Re" and "Im" denote the real and imaginary parts of a complex quantity. The full electromagnetic dispersion relation[11] with finite Larmor radius terms is very complicated and usually requires numerical treatment. However, rough estimates can be obtained analytically from approximate wave dispersion relations. For lower hybrid waves in the electrostatic approximation, the wave dispersion relation in a plasma with $\omega_{pe}^2 \ll \omega_{ce}^2$ is:

$$n_\perp^2 = -\frac{K_{zz}}{K_{xx}}\left(n_\parallel^2 - K_{xx}\right) , \tag{2a}$$

where

$$K_{xx} = 1 + \sum_\alpha \frac{\omega_{p\alpha}^2}{\omega k_\parallel v_{T\alpha}} \frac{e^{-\lambda_\alpha}}{\lambda_\alpha} \sum_{n=1}^{\infty} n^2 I_n \left(Z_n + Z_{-n}\right) , \tag{2b}$$

$$K_{zz} = 1 - \sum_\alpha \frac{\omega_{p\alpha}^2}{k_\parallel^2 v_{T\alpha}^2} e^{-\lambda_\alpha} \left[I_o Z_o' + \right.$$

$$\left. \sum_{n=1}^{\infty} I_n \left(\frac{\omega + n\omega_{c\alpha}}{\omega} Z_n' + \frac{\omega - n\omega_{c\alpha}}{\omega} Z_{-n}'\right)\right] . \tag{2c}$$

Subscript α denotes the particle species

T_α = temperature of the α-species,

m_α = mass of the α-species,

$\omega_{p\alpha}$ = plasma frequency of the α-species,

$\omega_{c\alpha}$ = cyclotron frequency of the α-species,

$$V_{Te} = \left(\frac{2T_\alpha}{m_\alpha}\right)^{1/2} ,$$

$$\lambda_\alpha = k_\perp^2 \rho_\alpha^2 = V_{T\alpha}^2/2\,\omega_{c\alpha}^2 ,$$

$I_n = I_n(\lambda_\alpha)$ is the modified Bessel function,

Z is the plasma dispersion function,

$$Z_n = Z\left[(\omega + n\,\omega_{c\alpha})/k_\parallel V_{T\alpha}\right] = Z(\zeta_n)$$

$$Z_n' = \frac{dZ_n}{d\,\zeta_n} .$$

For cold ions, $\omega/k_\parallel V_{Ti} >> 1$ and $k_\perp \rho_i << 1$. We can then expand $I_n(\lambda)$ in a power series in λ, keep terms of order λ, i.e., neglect terms containing $I_n(\lambda)$ with $|n| > 1$, and then obtain the cold ion wave dispersion relation. It is interesting to note that for $\omega >> \omega_{ci}$, the cold ion wave dispersion relation is the same as that derived from the assumption of unmagnetized ions ($\rho_i \to \infty$). Keeping terms of order λ^2, i.e., neglecting terms containing $I_n(\lambda)$ with $|n| > 2$, yields the first finite-Larmor-radius correction terms. This warm ion dispersion relation is generally used in the analysis of linear mode conversion[10] as well as in many ray tracing calculations.[12-15] In our previous paper,[18] we kept $I_n(\lambda)$ terms up to $|n| \sim 10$ which was sufficiently accurate for modest values of $k_\perp \rho_i$. However, in hot tokamak plasmas, $k_\perp \rho_i$ can be quite large and one needs to keep terms of $I_n(\lambda)$ until $e^{-\lambda} I_n(\lambda)$ becomes very small. In particular, for lower hybrid waves near the cold lower hybrid resonance layer, one should keep the $I_n(\lambda)$ terms at least up to $|n| \gtrsim \omega/\omega_{ci} \sim 50$. This retention is necessary because lower hybrid waves convert into hot

plasma waves and ion Bernstein waves[10,16] with very large $k_\perp$. Truncating at $n < \omega/\omega_{ci}$, the ion Bernstein wave is excluded from the picture and ion cyclotron damping is not properly accounted for.

Proceeding now to the calculation of wave damping, from Eq. (1b),

$$\frac{\mathrm{Im}(k_\perp)}{\mathrm{Re}(k_\perp)} \sim \frac{\left[\mathrm{Re}\,(K_{zz}) - (\mathrm{Re}\,n_\perp)^2\right] \mathrm{Im}\,(K_{xx}) - \left[n_\parallel^2 - \mathrm{Re}\,(K_{xx})\right] \mathrm{Im}\,(K_{zz})}{2\ \mathrm{Re}\,(K_{xx})\ (\mathrm{Re}\,n_\perp)^2} \,. \qquad (3)$$

Ion cyclotron harmonic damping effects show up predominantly in K_{xx} while electron Landau damping appears mainly in K_{zz}. The imaginary part of K_{xx} comes from the plasma dispersion function[17] $Z\,(\zeta_{-n})$. Since $\mathrm{Im}\,[Z\,(\zeta_{-n})] = \sqrt{\pi}\,\exp\,(-\zeta_{-n}^2)$ and $(\omega_{c\alpha}/k_\parallel\, V_{T\alpha})^2 \gg 1$ for ions, the single value of n which is closest to $\omega/\omega_{c\alpha}$ dominates. For the time being let n denote that particular value so that

$$\mathrm{Im}\,(K_{xx}) \simeq n^2 \frac{\omega_{p\alpha}^2}{\omega\, k_\parallel\, V_{T\alpha}} \frac{e^{-\lambda_\alpha} I_n(\lambda_\alpha)}{\lambda_\alpha} \sqrt{\pi}\, \exp\left[-\left(\frac{\omega - n\,\omega_{c\alpha}}{k_\parallel\, V_{T\alpha}}\right)^2\right] . \qquad (4a)$$

Representative parameters for a reactor environment might be $n_e = 2 \times 10^{14}$ cm^{-3}, B = 50 kG, and T = 15 keV. Substituting these FED (Fusion Engineering Device) parameters[18] into Eqs. (3) and (4), one finds that ICHD can be very strong for the lower hybrid wave even before it converts into an ion Bernstein wave. Since $\omega_{c\alpha}/k_\parallel\, V_{T\alpha} \gg 1$, Im (K_{xx}) is very sensitive to the value of $(\omega - n\,\omega_{c\alpha})$. The average value of Im (K_{xx}) can be obtained by integrating over ω from $(n-1/2)\,\omega_{c\alpha}$ to $(n+1/2)\,\omega_{c\alpha}$ which yields:

$$\langle \mathrm{Im}\,(K_{xx}) \rangle = n^2 \pi \frac{\omega_{p\alpha}^2}{\omega\,\omega_{c\alpha}} \frac{e^{-\lambda} I_n(\lambda_\alpha)}{\lambda_\alpha} \tag{4b}$$

From Eq. (4b), it can be shown that the maximum value of $\langle \mathrm{Im}\,(k_\perp)/\mathrm{Re}\,(k_\perp) \rangle$ can be of order unity when $\omega \sim \omega_{p\alpha}$. It should be noted that the above calculations are only rough estimates on wave damping. We have assumed $\omega_{pe}^2 \ll \omega_{ce}^2$ so that K_{xy} does not appear in the dispersion relation. We have also neglected terms which contain $dK_{xx}/dk_\perp$ and $dK_{zz}/dk_\perp$. At peak plasma density, $\omega_{pe}^2 \sim 0.5\ \omega_{ce}^2$ and terms containing K_{xy} should be retained. All these quantitative details are included in our numerical ray tracing code.

To investigate this effect more quantitatively, we have used a numerical ray tracing code to follow the lower hybrid wave in the FED plasma. The ray tracing code contains the hot plasma dielectric tensor and the electromagnetic terms as described previously.[18] However, in the dispersion relation, we now keep $I_n(\lambda)$ terms up to $|n| = 70$ or 100. The Bessel function subroutine[19] was carefully checked for $|n| \leq 100$, $\lambda \leq 100$. The low-q FED parameters ($q = 1.8$ at the plasma edge) are used as in the previous paper.[18] Figure 1 shows the absorption region (solid line) of lower hybrid waves at various frequencies. The lower hybrid resonance layer exists inside the plasma when $f \lesssim 1.4$ GHz. A fraction of the wave energy can still be absorbed by the ions when the wave frequency is only slightly above 1.4 GHz. When $f < 1.4$ GHz, as expected, practically all the wave energy is absorbed by the ions near a cyclotron harmonic layer. One would get approximately correct results if one simply were to use the warm ion dispersion relation to locate the mode conversion layer and then assume total absorption of the wave power by ions at this layer via ion Landau damping.[20] This is because the warm-ion dispersion

relation is still approximately valid for $k_\perp \rho_i >> 1$ provided that $\omega/k_\perp >> v_{Ti}$.[19] At frequencies above 1.7 GHz, electron Landau damping always dominates. At very high frequencies (up to 10 GHz), $n_\parallel$ increases as the wave propagates into the plasma and the wave is absorbed by electrons at $r > 80$ cm instead of going through a radial reflection as shown in the previous paper.[18] This change shows that the use of a more accurate wave dispersion relation can change the ray trajectories. It is also interesting to note that when we drop the high order $I_n(\lambda)$ terms, the resulting approximate wave dispersion relation incorrectly allows a slow wave solution even when the plasma density is slightly above the value for lower hybrid resonance. Inclusion of the high order $I_n(\lambda)$ terms brings in ion cyclotron damping and also corrects the real part of the dispersion relation at the same time.

The results shown in Fig. 1 were obtained for waves launched from the low field side ($\theta = 0$) of the tokamak. Ray tracing for other launching angles ($\theta = \pi/2$, π, $3\pi/2$) was also carried out for 1.4 GHz, 1.7 GHz, and 2.6 GHz waves and reveal no significant improvement. Good wave penetration occurs for lower plasma density ($n_o = 10^{14}$ cm^{-3}) and temperature ($T_o = 10$ keV) as shown by the dotted line in Fig. 1. Of course, with these parameters, the fusion power output will be substantially reduced. Generally speaking, good penetration for lower hybrid waves requires low density, low temperature, and high magnetic field (which implies a low β-value). In order to design a steady-state tokamak reactor sustained by lower hybrid waves, a careful investigation is necessary to identify a self-consistent set of plasma parameters which is compatible with all the engineering requirements and permits good wave penetration at the same time.

The fast wave dispersion relation in the lower hybrid frequency range can be approximated by the following:

$$n_\perp^2 = \frac{(K_{xy}')^2 - (n_\parallel^2 - K_{xx})^2}{n_\parallel^2 - K_{xx} + (K_{xy}')^2/K_{zz}} \tag{5}$$

where

$$K_{xy}' = -i\,K_{xy} = \sum_\alpha \frac{\omega_{p\alpha}^2}{\omega\, k_\parallel\, v_{T\alpha}}\, e^{-\lambda_\alpha} \sum_{n=1}^{\infty} n\,(I_n - I_n')\,(Z_n - Z_{-n})\ .$$

Wave propagation requires Re $(n_\perp^2) > 0$. For a cold plasma, $K_{xx} = 1 + \omega_{pe}^2/\omega_{ce}^2 - \omega_{pi}^2/\omega^2$, $K_{xy}' = \omega_{pe}^2/\omega\,\omega_{ce}$, $K_{zz} = 1 - \omega_{pe}^2/\omega^2$. Substituting these into Eq. (5), we can easily see that fast waves have to tunnel through an evanescent layer at the plasma edge. They begin to propagate when $\omega_{pe}^2 > (n_\parallel^2 - 1)\,\omega\,\omega_{ce}$. For $n_\parallel \sim 1.2$, the evanescent layer is thicker than that for slow waves which propagate when $\omega_{pe}^2 > \omega^2$. After the wave penetrates into the plasma, $K_{xy}' >> n_\parallel - K_{xx}$ and one can show that

$$\frac{\mathrm{Im}\,(k_\perp)}{\mathrm{Re}(k_\perp)} \sim \frac{\mathrm{Im}\,(K_{xx}) + \mathrm{Im}\,(K_{zz}) \cdot (\mathrm{Re}\,K_{xy}')^2/(\mathrm{Re}\,K_{zz})^2}{2\,[n_\parallel^2 - \mathrm{Re}\,(K_{xx}) + (\mathrm{Re}\,K_{xy}')^2/\mathrm{Re}\,(K_{zz})]}\ . \tag{6}$$

The Im K_{xx} term corresponds to ICHD and the Im K_{zz} term again corresponds to ELD. From Eqs. (3) and (6), one can make a comparison of the ICHD rate between fast and slow waves. For FED parameters, the value of λ for fast waves is typically several times smaller than it is for lower hybrid waves, which results in a smaller damping rate. Ray tracing calculations show that

the ion cyclotron damping rate for fast waves is usually smaller than the electron Landau damping rate, but it is not always negligible. Figure 2 displays the wave absorption region at various frequencies for outside launching ($\theta = 0$) and top launching ($\theta = \pi/2$) for the low-q FED parameters.[18] At high frequencies ($f > 1.5$ GHz), fast waves are absorbed at the plasma edge via electron Landau damping. Such behavior is quite similar to the slow wave. At low frequencies ($f < 1$ GHz), fast waves can reach the plasma center, undergo a radial reflection and propagate back out with negligible absorption. This is qualitatively the same result as published previously.[18] However, there is one important difference: there is a narrow frequency window in which strong absorption in a single pass, with good penetration, is possible. This difference is due to the high order terms $I_n(\lambda)$ retained in the present calculation. Typical features of fast wave behavior are displayed in Fig. 3. At 1.44 GHz, the fast wave radial group velocity is very low at the plasma edge, resulting in rapid oscillations in $n_\parallel$ and $k_\perp$ as shown in Fig. 3a and Fig. 3b. Figure 3c shows that 60% of the wave energy is absorbed in this region ($r > 80$ cm) via electron Landau damping. As the wave propagates towards the center, $k_\perp$ increases with the plasma density and ICHD can become important at the cyclotron harmonic layers. Figure 3d shows the spatial damping rate due to electrons (Im $k_{\perp e}$) and ions (Im $k_{\perp i}$) as a function of plasma radius. The variation of Im $k_{\perp e}$ is mainly due to the change of $n_\parallel$, or more precisely, $\omega/k_\parallel v_{Te}$. The maxima of Im $k_{\perp e}$ corresponds to the maxima of $n_\parallel$ while the peaks of Im $k_{\perp i}$ are located where ω/ω_{ci} is an integer. Only some of the peaks are shown to illustrate that Im $k_{\perp i}$ is comparable to Im $k_{\perp e}$ at the cyclotron harmonic layers and a small fraction of wave energy is absorbed by the ions at each layer. At lower frequencies, the radial group velocity is higher as displayed in Fig. 4, and the waves can

penetrate easily into the plasma center. When a 1 GHz fast wave is launched from the top ($\theta = \pi/2$), strong absorption in one transit can be achieved with a very good absorption profile. Since $k_\perp$ is smaller at lower frequencies, Im $k_{\perp i}$ is always much smaller than Im $k_{\perp e}$ as shown in Fig. 5d. Therefore, ion absorption is negligible in this case. It should be pointed out that the strong absorption for waves launched at $\theta = \pi/2$ is a consequence of large $n_\parallel$ which reaches 1.6 along its trajectory. When the wave is launched at $\theta = \pi$, $n_\parallel$ goes up to 2.0 and the wave is totally absorbed before it reaches the plasma center. Wave absorption at large $n_\parallel$ is not desirable from the efficiency point of view because the generated current is carried by the slow electrons which are more collisional.

As mentioned earlier, we observe rays with a good absorption profile only when we use the more accurate dispersion relation in which high order terms of $I_n(\lambda)$ are retained. Figure 6 shows the calculated absorption region for 1 GHz fast waves when different orders of $I_n(\lambda)$ are kept in the hot plasma dielectric tensor. It is apparent that the truncation point N can be important. When N is large enough, $e^{-\lambda} I_n(\lambda)$ becomes very small for $n > N$, terms of order $n > N$ are unimportant, and the computed result becomes independent of N. As displayed in Fig. 6, the absorption region for N = 70 is identical to that for N = 100; the computed values for all the quantities agree within three digits at least. When we truncate at $N \leq 10$, the results are significantly different. This shows that the high order terms of $I_n(\lambda)$ can make a significant contribution to the wave dispersion relation.

III. ALPHA-PARTICLE DAMPING

In the previous section, we analyzed ICHD of slow and fast waves due to 15 keV Maxwellian deuterium and tritium ions. Strong damping can occur when λ

$= k_\perp^2 \rho_i^2$ is large. The alpha particles produced at an energy of $E_o = 3.5$ MeV have a much larger Larmor radius which may result in strong wave damping. In order to calculate the damping rate, we need to know the α-particle distribution function $f_\alpha(\vec{v})$. The initial α-particle velocity is $v_o = 1.3 \times 10^9$ cm/sec. Since $v_{Te} >> v_o >> v_{Ti}$, they are mainly slowed down by the electron drag, and the slowing down time τ_s is not sensitive to the α-particle energy until its energy drops down to a value E_1 comparable to the ion temperature. Wave damping is mainly due to the energetic particles with energy above E_1. For unpolarized ions, the α-particles are created isotropically in velocity space and remain isotropic as they slow down. From particle conservation, we get:

$$E \cdot n_\alpha (E)\, e^{-t/\tau_s} = (E + \Delta E) \cdot n_\alpha (E + \Delta E)\, e^{-t/\tau_s} ,$$

$$\Delta \left[E \cdot n_\alpha (E) \right] = 0 ,$$

$$n_\alpha (E) = \frac{A\, n_e}{E} ,$$

where $n_\alpha(E)$ is the α-particle density at energy $E = 1/2\ m_\alpha v^2$, n_e is the electron density, and A is a constant which depends on the fusion cross section. The α-particle density with energy between E_1 and E_0 is:

$$n_{\alpha T} = \int_{E_1}^{E_0} \frac{A\, n_e}{E}\, d E = A\, n_e\, \ell n \left(\frac{E_o}{E_1}\right) \sim 5\, A\, n_e .$$

It is apparent that $n_{\alpha T}$ is not too sensitive to E_1 because of the logorithm: we have put $E_1 \sim 30$ keV. Let σ denote the fusion cross section, n_D and n_T denote the deuterium and tritium density, and the α-particle production rate per unit volume is $\langle\sigma v\rangle\, n_D\, n_T$. At steady state,

$$\frac{d}{dt} n_{\alpha T} = 0 = \langle\sigma v\rangle\, n_D\, n_T - \frac{n_{\alpha T}}{\tau_s} ,$$

which yields

$$A = \frac{\langle\sigma v\rangle\, n_e\, \tau_s}{20} \tag{7}$$

and

$$f_\alpha\,(v_\perp, v_\parallel) = \frac{A\, n_e}{2\pi\left(v_\perp^2 + v_\parallel^2\right)^{3/2}} . \tag{8}$$

We would like to stress the fact that Eq. (8) is a valid approximation only for the energetic tail of the α-particle distribution function where τ_s is independent of E, but this is the part that is vital to wave damping. For $n_e = 2 \times 10^{14}$ cm^{-3}, $T_e = T_i = 15$ keV, we have $\tau_s \sim 1.3$ sec, $n_{\alpha T} \sim 3 \times 10^{12}$ cm^{-3}, and the average kinetic energy of the α-particle is; $T_\alpha = 0.33$ MeV. The contribution of these α-particles to K_{xx} is[11]:

$$(K_{xx})_\alpha = \frac{1}{n_{\alpha T}} \frac{2\pi}{\omega} \frac{\omega_{p\alpha}^2}{\omega_{c\alpha}} \sum_n \int_L dv_\parallel \int_0^\infty dv_\perp \frac{2v_\perp n^2 \omega_{c\alpha}^3}{k_\perp^2}$$

$$\frac{J_n^2 \left(\frac{k_\perp v_\perp}{\omega_{c\alpha}}\right) \left[\frac{\partial f_\alpha}{\partial v_\perp^2}\left(1 - \frac{k_\parallel v_\parallel}{\omega}\right) + \frac{k_\parallel v_\parallel}{\omega} \frac{\partial f_\alpha}{\partial v_\parallel^2}\right]}{k_\parallel v_\parallel + n\omega_{c\alpha} - \omega} \quad . \tag{9}$$

Integrate over $v_\parallel$ along the Landau contour to get the imaginary part of Eq. (9):

$$\mathrm{Im}\,(K_{xx})_\alpha = -\frac{3\pi}{5} \frac{1}{|k_\parallel|} \frac{\omega_{p\alpha}^2}{\omega\,\omega_{c\alpha}} \sum_n \frac{n^2 \omega_{c\alpha}^3}{k_\perp^2} \int_0^\infty \frac{J_n^2\left(\frac{k_\perp v_\perp}{\omega_{c\alpha}}\right) v_\perp\, dv_\perp}{\left[v_\perp^2 + \left(\frac{\omega - n\omega_{c\alpha}}{k_\parallel}\right)^2\right]^{5/2}} \quad . \tag{10}$$

When $\omega = n\omega_{c\alpha}$, we get[21]

$$\int_0^\infty \frac{J_n^2\left(\frac{k_\perp v_\perp}{\omega_{c\alpha}}\right) v_\perp\, dv_\perp}{\left[v_\perp^2 + \left(\frac{\omega - n\omega_{c\alpha}}{k_\parallel}\right)^2\right]^{5/2}} \simeq \int_0^\infty \frac{J_n^2\left(\frac{k_\perp v_\perp}{\omega_{c\alpha}}\right)}{v_\perp^4}\, d\, v_\perp$$

$$= \left(\frac{k_\perp}{\omega_{c\alpha}}\right)^3 \frac{\Gamma(4)\,\Gamma\left(\frac{2n-3}{2}\right)}{2^4\,\Gamma\left(\frac{5}{2}\right)\,\Gamma\left(\frac{2n+5}{2}\right)\,\Gamma\left(\frac{5}{2}\right)} \quad .$$

Substitute this into Eq. (10) and get

$$\mathrm{Im}\,(K_{xx})_\alpha \simeq -\frac{2}{5n^2} \cdot \frac{\omega_{p\alpha}^2}{\omega\,\omega_{c\alpha}} \frac{k_\perp}{|k_\parallel|} \quad . \tag{11}$$

This is the maximum value evaluated at $\omega = n\omega_{c\alpha}$. The average value $\langle \mathrm{Im}\,(K_{xx})_\alpha \rangle$ obtained numerically is lower by a factor of 2 to 4, depending on the values of $n, k_\parallel$ and $k_\perp$. The damping rate for lower hybrid waves due to the energetic α-particles is:

$$\mathrm{Im}\,(k_{\perp\alpha}) \sim \frac{k_\perp \left[\mathrm{Re}(K_{zz}) - (\mathrm{Re}\; n_\perp)^2\right] \langle \mathrm{Im}\,(K_{xx})_\alpha \rangle}{2\;\mathrm{Re}\,(K_{xx})\,(\mathrm{Re}\; n_\perp)^2} \quad . \tag{12}$$

For PED parameters with $k_\perp \sim 20\ \mathrm{cm}^{-1}$, $f \sim 1.7\ \mathrm{GH_z}$, $n_\parallel \sim 1.4$,

$$\mathrm{Im}\,(k_{\perp\alpha}) \sim 10^{-2}\, k_\perp \sim 0.2\ \mathrm{cm}^{-1} \ ,$$

and the absorption length is:

$$L_\alpha \sim \frac{1}{\mathrm{Im}(k_{\perp\alpha})} \sim 5\ \mathrm{cm} \quad .$$

The damping rate for fast waves due to the energetic α-particles is:

$$\mathrm{Im}\,(k_{\perp\alpha}) \sim \frac{k_\perp \; < \mathrm{Im}(K_{xx})_\alpha >}{2\,[n_\parallel^2 - \mathrm{Re}(K_{xx}) + (\mathrm{Re}\,K_{xy}')^2/\mathrm{Re}(K_{zz})]} \quad . \tag{13}$$

For FED parameters with $k_\perp \sim 10\ \mathrm{cm}^{-1}$, $f \sim 1.2\ \mathrm{GHz}$, $n_\parallel \sim 1.4$,

$$\mathrm{Im}\,(k_{\perp\alpha}) \sim 1.2 \times 10^{-2}\, k_\perp \sim 0.12\ \mathrm{cm}^{-1} \quad ,$$

and the absorption length L_α is:

$$L_\alpha \sim \frac{1}{\mathrm{Im}(k_{\perp\alpha})} \sim 8\ \mathrm{cm} \quad .$$

It should be noted here that the above calculation assumes a uniform magnetic field, i.e., we assume that the unperturbed α-particle orbit is a helix. For a 300 keV α-particle in a 50 kG magnetic field, the Larmor radius is about 2 cm which is comparable to the distance between neighboring cyclotron harmonic layers in FED. Therefore, the uniform field assumption may not be a very good approximation. We can also estimate $(K_{xx})_\alpha$ by assuming unmagnetized[20] α-particles and get:

$$(K_{xx})_\alpha = -\frac{\omega_{p\alpha}^2}{k^2} \int_L \frac{dF(u)}{u - \omega/k}\, du \quad , \tag{14}$$

where $F(u) = \int f_\alpha(\vec{v})\, \delta\left(u - \frac{\vec{k}\cdot\vec{v}}{k}\right) d\vec{v}$.

Use Eq. (8) for $f_\alpha(\vec{v})$ to obtain $F(u) = (5u)^{-1}$ and

$$\mathrm{Im}\left(K_{xx}\right)_\alpha = \frac{\pi}{5}\frac{\omega_{p\alpha}^2}{\omega^2} \quad . \tag{15}$$

If we assume $n_{\alpha T} = 3 \times 10^{12}$ cm^{-3}, $k \sim 20$ cm^{-1} for 1.7 GHz lower hybrid waves, we get $\mathrm{Im}(k_{\perp\alpha}) \sim 0.6$ cm^{-1}. The same value of $\mathrm{Im}(k_{\perp\alpha})$ is obtained for a 1.2 GHz fast wave with $k \sim 10$ cm^{-1}. The temporal damping rate γ can be estimated from $\gamma = \omega\ \mathrm{Im}\ k_\perp / \mathrm{Re}\ k_\perp > \omega_{c\alpha}$ which justifies the assumption of straight α-particle orbits.[22] These values are comparable to the previous estimates based on helical α-particle orbits. It should be pointed out that the alpha particle density $n_{\alpha T}$ is calculated from the peak plasma density and temperature. Yet the damping is so strong that even if we lower $n_{\alpha T}$ by a factor of ten, they can still be a major obstacle for rf current drive in the lower hybrid frequency range. This problem is similar to that recently predicted for low frequency (much lower than lower hybrid frequency) fast wave current drive via electron transit-time-magnetic-pumping.[23]

IV. SUMMARY

In this paper we calculate analytically as well as numerically the effect of ICHD on slow and fast waves used for current drive near the lower hybrid frequency. As expected, one has to use slow waves above the lower hybrid resonance frequency to avoid ion absorption. We cannot find a lower

hybrid wave that can reach the plasma center with the low-q FED parameters. ICHD is usually much weaker for fast waves because $k_\perp$ is smaller. For fast waves in the FED parameters, $k_\perp$ can reach 20 cm^{-1} at frequencies above 1.2 GHz and ICHD can be comparable to electron Landau damping near a cyclotron harmonic layer. However, the majority of the wave energy still goes into electrons. It is important to note that the high order terms of $I_n(\lambda)$ in the dielectric tensor can make a significant contribution to the real part of the wave dispersion relation. By keeping terms up to $n \geq \omega/\omega_{ci}$, the consequent ray trajectories can be quite different from calculations which truncate at $n < \omega/\omega_{ci}$. Calculated wave penetration becomes worse for slow waves and better for fast waves when higher order terms are retained. Single-pass absorption near the plasma center becomes possible for fast waves in the frequency range of 1 - 1.4 GHz. These waves look very promising for current drive in tokamak reactors until we consider the α-particle effects. Analytic estimates indicate that both the fast and the slow waves will be absorbed by the α-particles. In order to sustain a steady-state tokamak with waves in the lower hybrid frequency range, one may have to remove the energetic alpha particles before they thermalize with the plasma and rely on the input wave power to maintain the plasma temperature after ignition. If the alpha particle problem cannot be overcome, then the application of lower hybrid wave current drive will be limited to current ramp-up before ignition.

ACKNOWLEDGMENTS

The authors would like to thank F.W. Perkins, T.H. Stix, F. Skiff, and J. Minahan for helpful dicussions and assistance in the preparation of the manuscript. This work was supported by the U.S. Department of Energy Contract No. DE-AC02-76-CHO-3073.

REFERENCES

[1]N.J. Fisch, Phys. Rev. Lett. 41, 873 (1978).

[2]K.L. Wong, R. Horton, and M. Ono, Phys. Rev. Lett. 45, 117 (1980).

[3]T. Yamamoto, T. Imai, M. Shimada, N. Suzuki, M. Naeno, S. Konoshima, T. Fuzii, K. Uehara, T. Nagashima, A. Funahashi, and N. Fugisawa, Phys. Rev. Lett. 45, 716 (1980).

[4]S.C. Luckhardt, M. Porkolab, S.F. Knowlton, K.-I. Chen, A.S. Fisher, F.S. McDermott, and M. Mayberry, Phys. Rev. Lett. 48, 152 (1982).

[5]K. Ohkubo, S. Takamure, K. Kawahata, T. Tetsuka, K. Matsuura, N. Noda, K. Sakurai, S. Tanahashi, and J. Fujita, Nucl. Fusion 22, 203 (1982).

[6]S. Bernabei, C. Daughney, P. Efthimion, W. Hooke, J. Hosea, F. Jobes, A. Martin, E. Mazzucato, E. Meservey, R. Motley, J. Stevens, S. von Goeler, and R. Wilson, Phys. Rev. Lett. 49, 1255 (1982).

[7]M. Porkolab et al., in Plasma Physics and Controlled Nuclear Fusion Research (IAEA, Vienna, 1983), Vol. 1, p. 227.

[8]S. Kubo, M. Nakamure, T. Cho, S. Nakao, T. Shimozuma, A. Ando, K. Ogura, T. Maekawa, Y. Terumichi, and S. Tanaka, Phys. Rev. Lett. 50, 1994 (1983).

[9]D.A. Ehst, Nucl. Fusion 19, 1369 (1979).

[10]T.H. Stix, Phys. Rev. Lett. 15, 878 (1965).

[11]N.A. Krall and A.W. Trivelpiece, Principles of Plasma Physics (McGraw-Hill, New York, 1973) p. 405.

[12]D.W. Ignat, Phys. Fluids 24, 1110 (1981).

[13]Yu. F. Baranov and V.I. Fedorov, Nucl. Fusion 20, 1111 (1980).

[14]P.T. Bonoli and E. Ott, Phys. Fluids 25, 359 (1982).

[15]S. Bernabei and D.W. Ignat, Nucl. Fusion 22, 735 (1982).

[16]G.A. Wurden, K.L. Wong, F. Skiff, and M. Ono, Phys. Rev Lett. 50, 1779 (1983).

[17]B.D. Fried and S.D. Conte, The Plasma Dispersion Function (Academic Press, New York, 1961).

[18]K.L. Wong and M. Ono, Nucl. Fusion 23, 805 (1983).

[19]The Bessel function subroutine employs the backward recurrence relation technique. We calculate $e^{-\lambda} I_n(\lambda)$ up to n = 100, λ = 100 in the CRAY computer and the returned values are checked with Abramowitz and Stegun, Handbook of Mathematical Functions, (Dover Publications, Inc., New York, 1970) p. 428. They agree up to 6 digits at least. It should be noted that

small computers (like PDP-10) can handle up to $\lambda = 50$. At $\lambda = 100$, the returned values are smaller by $10^4 - 10^5$. For approximate calculations, one can avoid computing the Bessel functions by using the approximate dispersion relation derived by M. Brambilla. (See M. Brambilla, Plasma Phys. 18, 669; also T.W. Tang, K.Y. Fu, and M.W. Farshori, Plasma Phys. 21, 127.)

[20]Mario D. Simonutti, Phys. Fluids 18, 1524 (1975).

[21]I.S. Gradshtyn and I.M. Ryzhik, Table of Integrals Series and Products, 4th ed. (Academic Press, New York, 1965) p. 692.

[22]D.E. Baldwin and G. Rowlands, Phys. Fluids 9, 2444 (1966).

[23]F.W. Perkins, in ORNL/FEDC - 83/1, Oak Ridge National Laboratory, Oak Ridge, Tennessee, (1983).

FIGURE CAPTIONS

FIG. 1 Absorption region of lower hybrid waves with the low-q FED parameters. The dotted line shows the absorption region at lower density ($n_o = 10^{14}$ cm^{-3}) and lower temperature ($T_o = 10$ keV). The waves are launched at $r_o = 120$ cm, $\theta_o = 0$ (outside launching) with $n_T = 1.2 = n_\parallel$. n_t is the index of refraction in the toroidal direction.

FIG. 2 Absorption region of fast waves with the low-q FED parameters. The waves are launched at $r_o = 116$ cm (to avoid the evanescent layer at the surface) with $n_t = 1.2$. (a) outside launching, $\theta_o = 0$. (b) top launching, $\theta_o = \pi/2$. The number at the reflection point represents the fraction of power remained in the wave when it undergoes reflection.

FIG. 3 Characteristics of 1.44 GHz fast waves launched at $r_o = 116$ cm, $\theta_o = 0$ with $n_t = 1.2$. (a) Variation of $n_\parallel$ with radial location. The dotted lines define the range within which $n_\parallel$ oscillates. (b) Variation of $k_\perp$ with radial location. $k_\perp$ oscillates between the dotted lines near the surface ($r > 90$ cm). (c) Power absorption profile. (d) Spatial damping rates by electrons (dotted curve) and ions (solid curve).

FIG. 4 Variation of radial group velocity with radial location for fast waves at different frequencies. The waves are launched at $r_o = 116$ cm, $\theta_o = 0$ with $n_t = 1.2$. The shaded area represents the region in which the group velocity of the 1.44 GHz fast wave oscillates.

FIG. 5 Characteristics of 1.0 GHz fast waves launched at r_o = 116 cm, $\theta_o = \pi/2$ with n_t = 1.2. (a) Variation of $n_\parallel$ with radial location. (b) Variation of $k_\perp$ with radial location. (c) Power absorption profile. (d) Spatial damping rates by electrons (dotted line) and ions (solid curve).

FIG. 6 Effects of high order Bessel functions in the dispersion relation on the characteristics of the fast wave launched at r_o = 116 cm with n_t = 1.2. (a) f = 1.0 GHz, θ_o = 0, (b) f = 1.0 GHz, $\theta_o = \pi/2$. The absorption region depends on the truncation point.

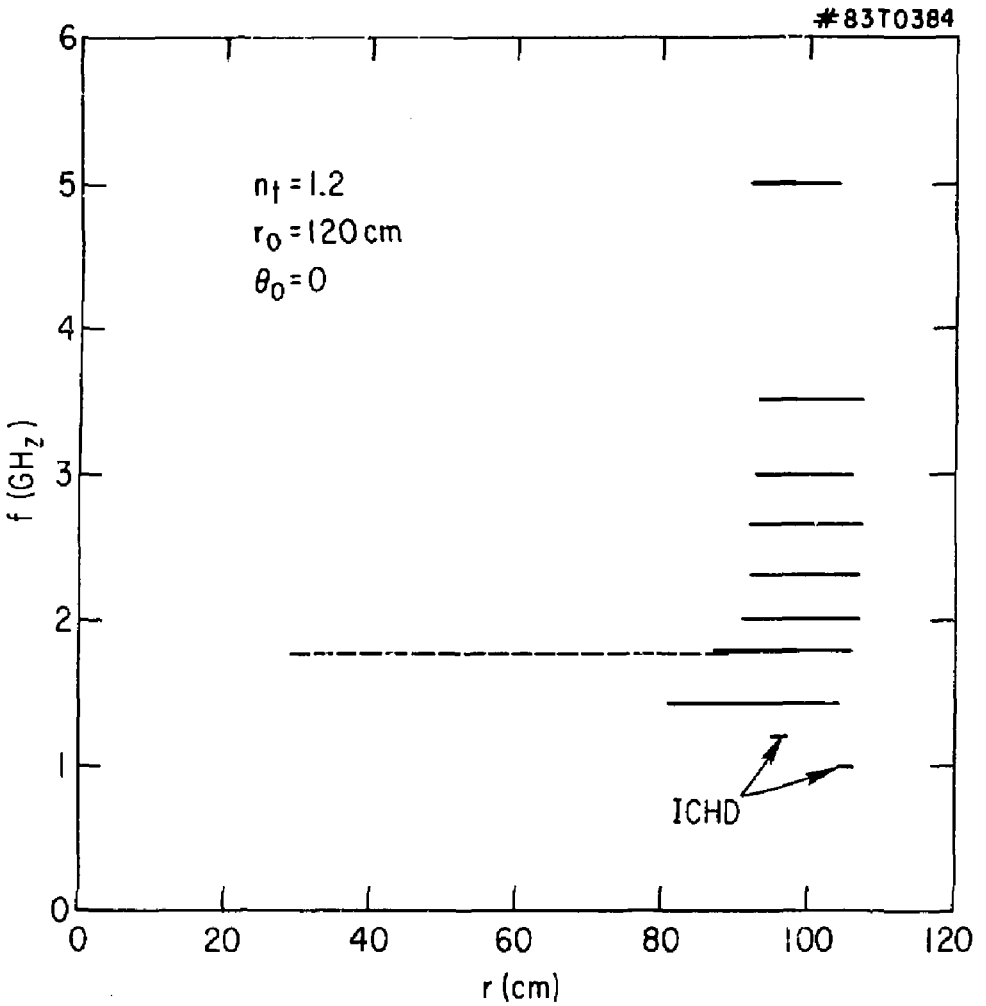
#83T0384
$n_f = 1.2$
$r_0 = 120\,cm$
$\theta_0 = 0$
ICHD
f (GHz)
r (cm)
0
1
2
3
4
5
6
0
20
40
60
80
100
120

Fig. 1

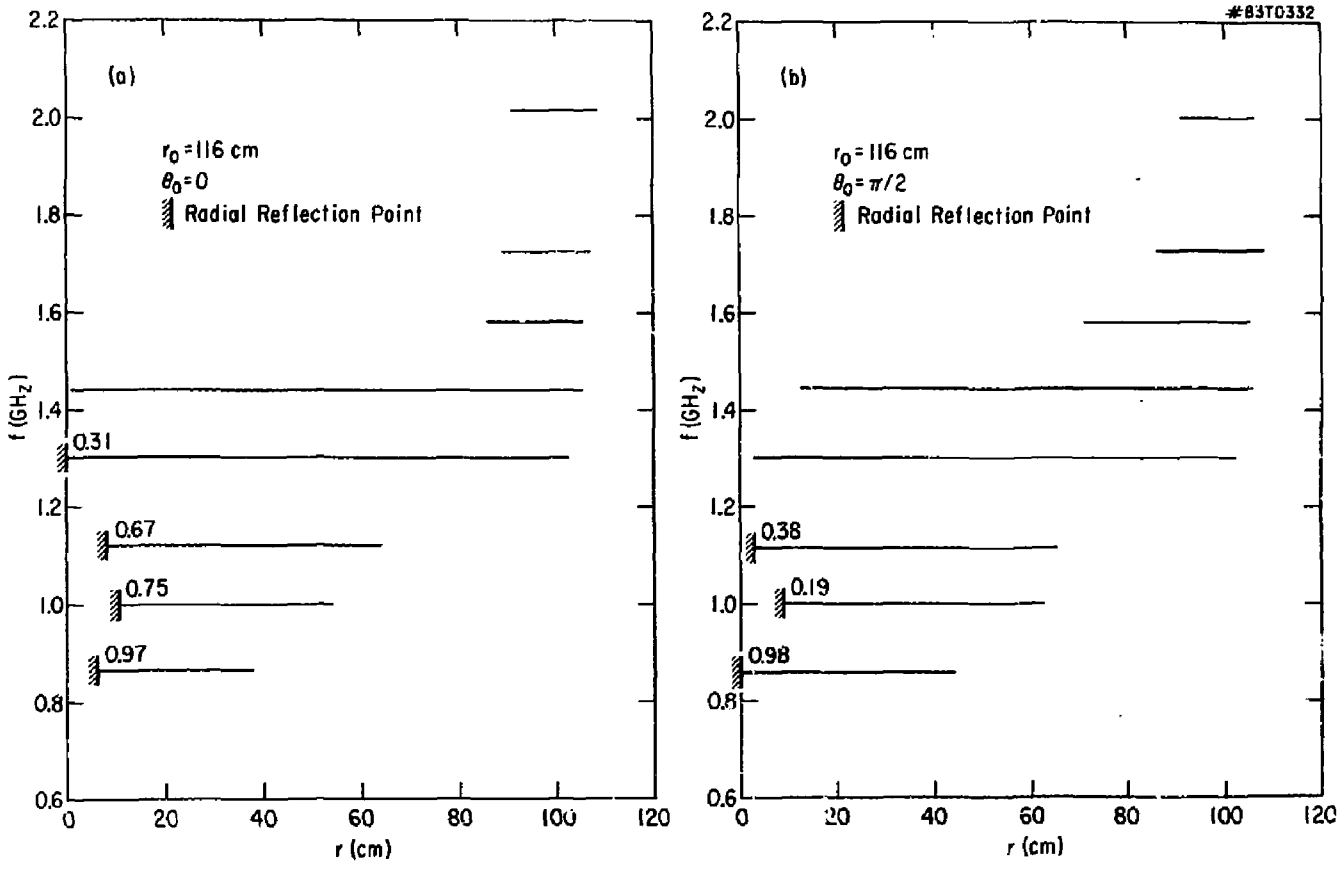
#83T0332
(a)
r_0 = 116 cm
θ_0 = 0
Radial Reflection Point
0.31
0.67
0.75
0.97
(b)
r_0 = 116 cm
$\theta_0 = \pi/2$
Radial Reflection Point
0.38
0.19
0.98
f (GHz)
r (cm)
2.2
2.0
1.8
1.6
1.4
1.2
1.0
0.8
0.6
0
20
40
60
80
100
120

Fig. 2

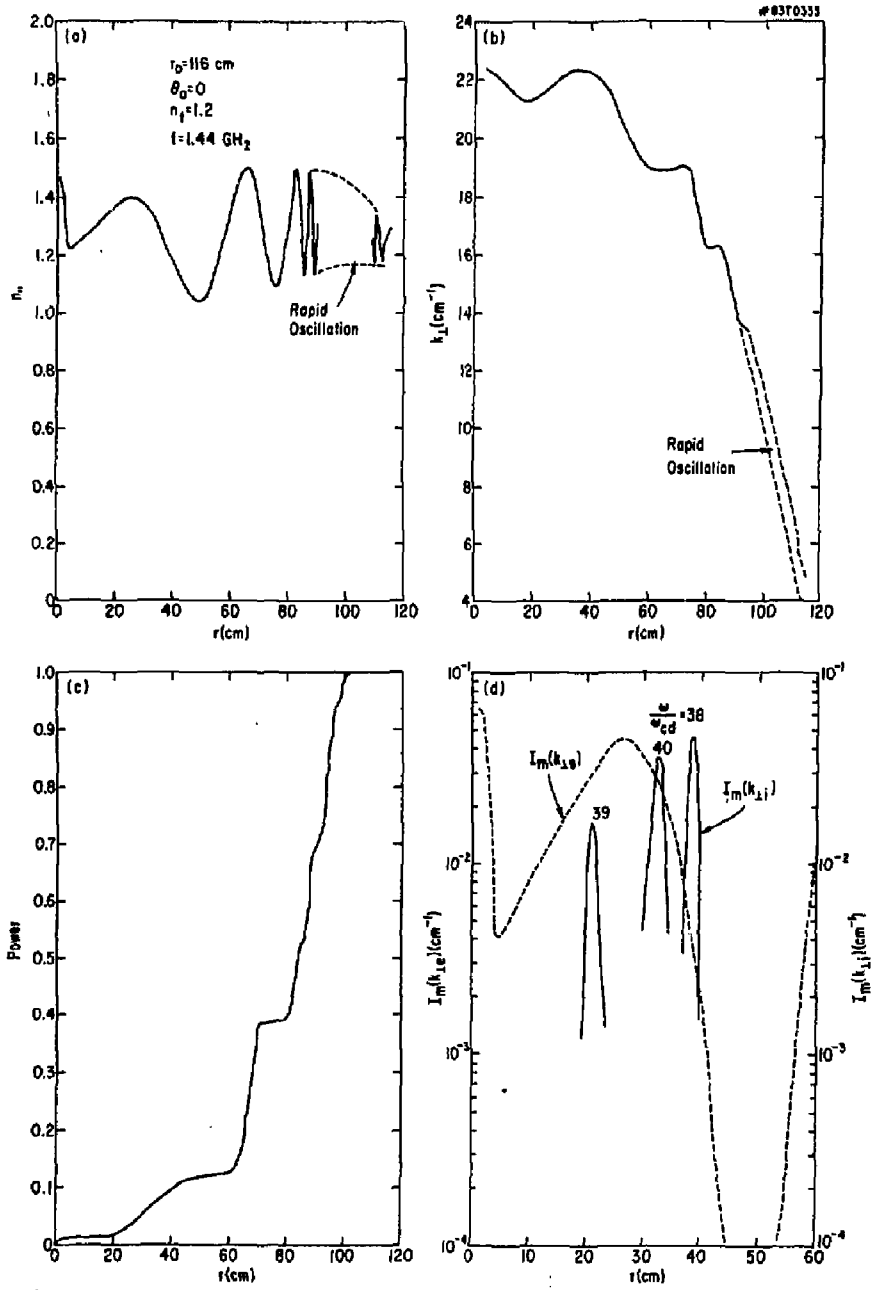
(a)
r_0=116 cm
θ_0=0
$n_\parallel$=1.2
f=1.44 GH$_z$
Rapid Oscillation
$n_\perp$
r(cm)
#83T0333
(b)
Rapid Oscillation
$k_\perp$(cm^{-1})
r(cm)
(c)
Power
r(cm)
(d)
$\frac{\omega}{\omega_{cd}}$=38
40
39
$I_m(k_{\perp e})$
$I_m(k_{\perp i})$
$I_m(k_{\perp e})$(cm^{-1})
$I_m(k_{\perp i})$(cm^{-1})
r(cm)

Fig. 3

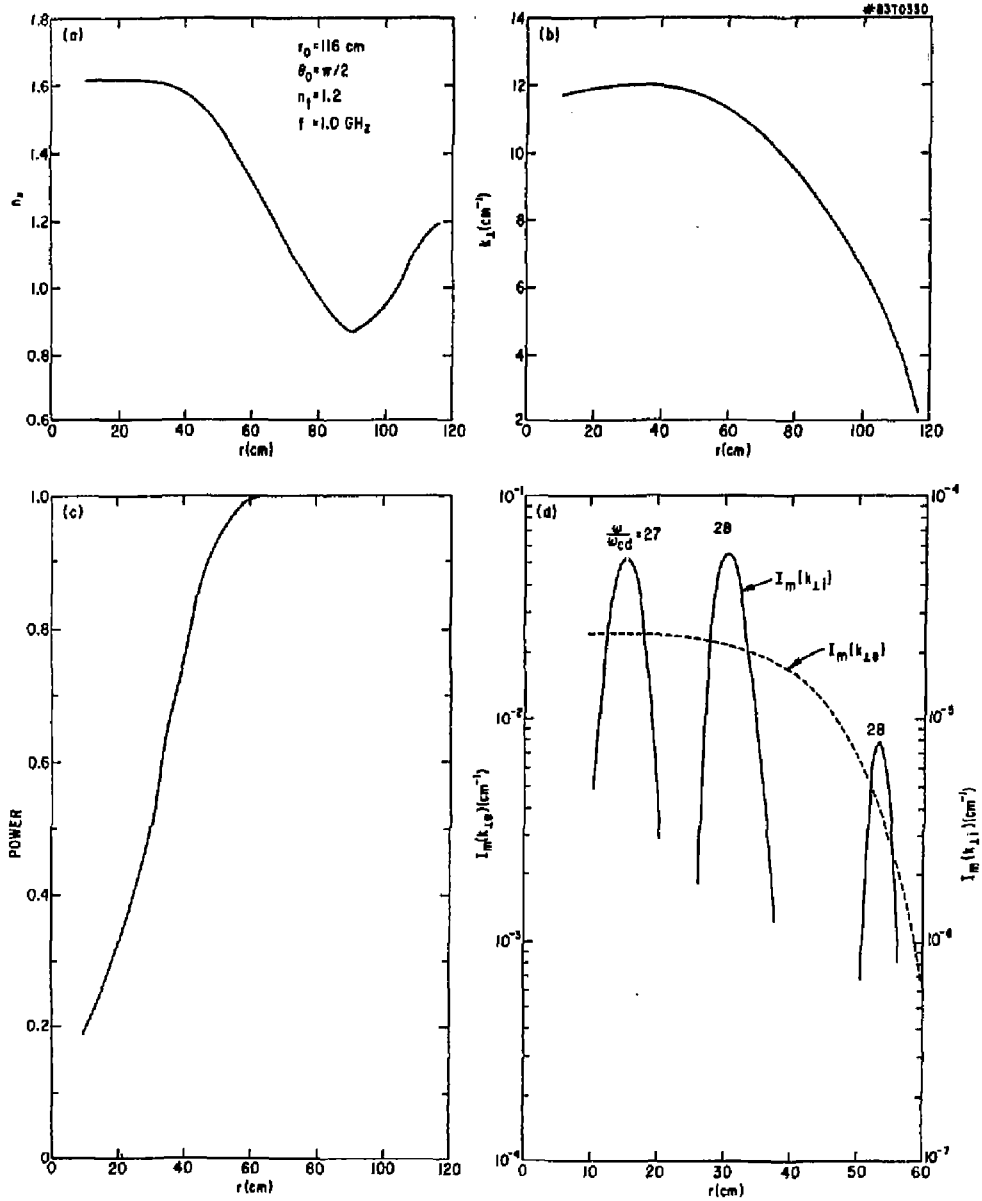
#8370330
(a)
r_0=116 cm
θ_0=π/2
$n_\parallel$=1.2
f =1.0 GHz
$n_\perp$
r(cm)
(b)
$k_\perp$(cm^{-1})
r(cm)
(c)
POWER
r(cm)
(d)
$\frac{\omega}{\omega_{cd}}$=27
28
$I_m[k_\perp]$
$I_m[k_{\perp e}]$
28
$I_m[k_{\perp e}]$(cm^{-1})
$I_m[k_\perp]$(cm^{-1})
r(cm)

Fig. 4

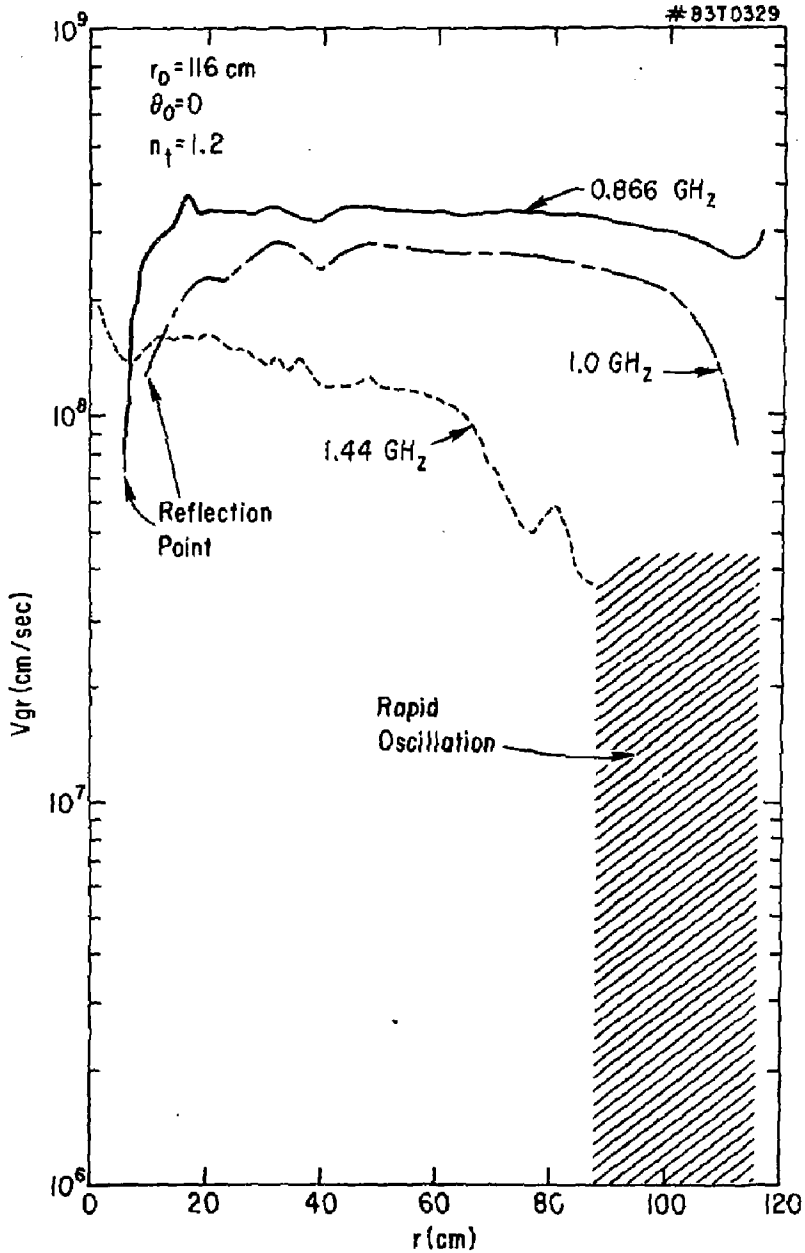
#8310329
r_0=116 cm
θ_0=0
n_t=1.2
0.866 GHz
1.0 GHz
1.44 GHz
Reflection Point
Rapid Oscillation
Vgr (cm/sec)
r(cm)
10^9
10^8
10^7
10^6
0
20
40
60
80
100
120

Fig. 5

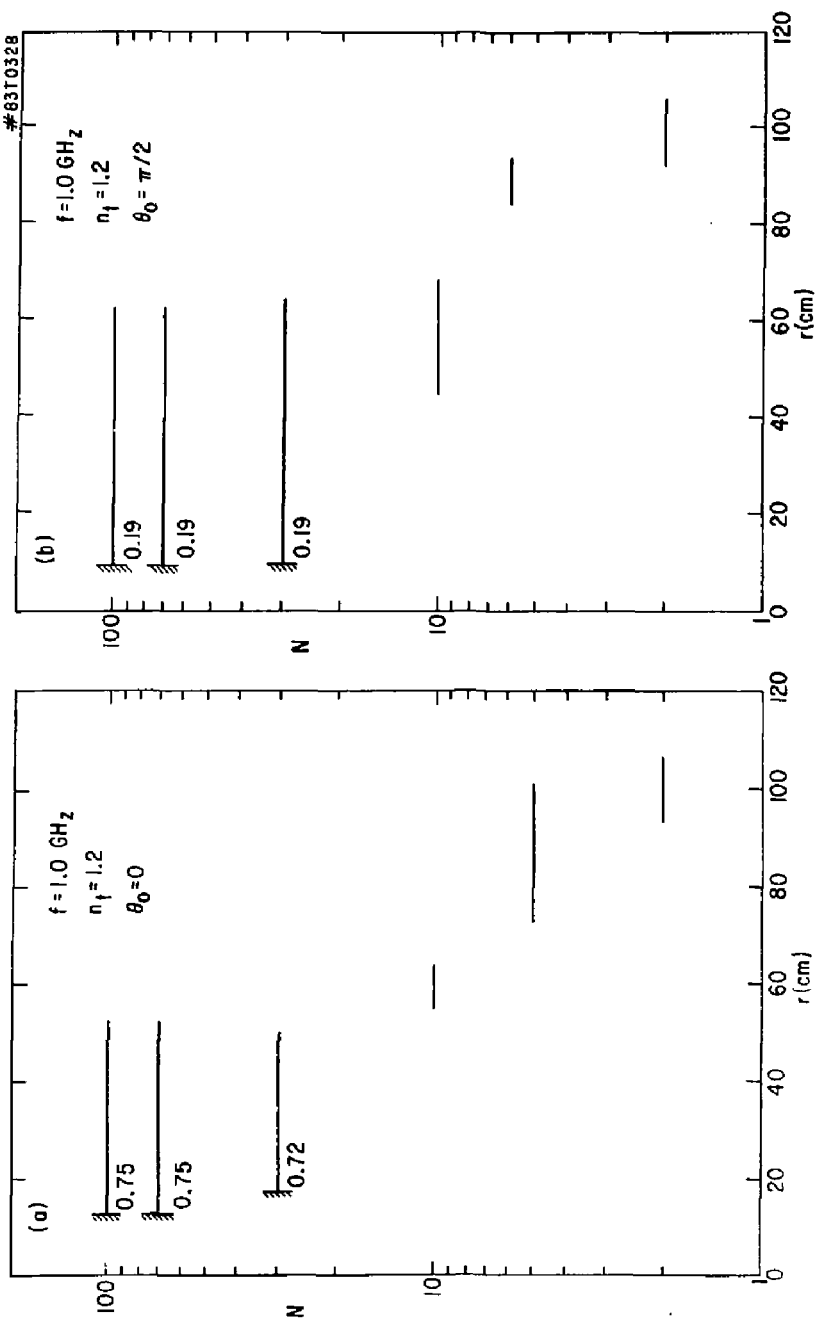
#83T0328
(a)
f=1.0 GHz
n_f=1.2
θ_0=0
0.75
0.75
0.72
N
r(cm)
(b)
f=1.0 GHz
n_f=1.2
θ_0=π/2
0.19
0.19
0.19
N
r(cm)

Fig. 6

EXTERNAL DISTRIBUTION IN ADDITION TO TIC UC-20

Plasma Res Lab, Austra Nat'l Univ, AUSTRALIA
Dr. Frank J. Paoloni, Univ of Wollongong, AUSTRALIA
Prof. I.R. Jones, Flinders Univ., AUSTRALIA
Prof. M.H. Brennan, Univ Sydney, AUSTRALIA
Prof. F. Cap, Inst Theo Phys, AUSTRIA
Prof. Frank Verheest, Inst theoretische, BELGIUM
Dr. C. Palumbo, Dg XII Fusion Prog, BELGIUM
Ecole Royale Militaire, Lab de Phys Plasmas, BELGIUM
Dr. P.H. Sakanaka, Univ Estadual, BRAZIL
Dr. C.R. James, Univ of Alberta, CANADA
Prof. J. Teichmann, Univ of Montreal, CANADA
Dr. H.M. Skarsgard, Univ of Saskatchewan, CANADA
Prof. S.R. Sreenivasan, University of Calgary, CANADA
Prof. Tudor W. Johnston, INRS-Energie, CANADA
Dr. Hannes Barnard, Univ British Columbia, CANADA
Dr. M.P. Bachynski, MPB Technologies, Inc., CANADA
Zhengwu Li, SW Inst Physics, CHINA
Library, Tsing Hua University, CHINA
Librarian, Institute of Physics, CHINA
Inst Plasma Phys, Academia Sinica, CHINA
Dr. Peter Lukac, Komenskeho Univ, CZECHOSLOVAKIA
The Librarian, Culham Laboratory, ENGLAND
Prof. Schatzman, Observatoire de Nice, FRANCE
J. Radet, CEN-BP6, FRANCE
AM Dupas Library, AM Dupas Library, FRANCE
Dr. Tom Mual, Academy Bibliographic, HONG KONG
Preprint Library, Cent Res Inst Phys, HUNGARY
Dr. S.K. Trehan, Panjab University, INDIA
Dr. Indra, Mohan Lal Das, Banaras Hindu Univ, INDIA
Dr. L.K. Chavda, South Gujarat Univ, INDIA
Dr. R.K. Chhajlani, Var Ruchi Marg, INDIA
P. Kaw, Physical Research Lab, INDIA
Dr. Phillip Rosenau, Israel Inst Tech, ISRAEL
Prof. S. Cuperman, Tel Aviv University, ISRAEL
Prof. G. Rostagni, Univ Di Padova, ITALY
Librarian, Int'l Ctr Theo Phys, ITALY
Miss Clelia De Palo, Assoc EURATOM-CNEN, ITALY
Biblioteca, del CNR EURATOM, ITALY
Dr. H. Yamato, Toshiba Res & Dev, JAPAN
Prof. M. Yoshikawa, JAERI, Tokai Res Est, JAPAN
Prof. T. Uchida, University of Tokyo, JAPAN
Research Info Center, Nagoya University, JAPAN
Prof. Kyoji Nishikawa, Univ of Hiroshima, JAPAN
Prof. Sigeru Mori, JAERI, JAPAN
Library, Kyoto University, JAPAN
Prof. Ichiro Kawakami, Nihon Univ, JAPAN
Prof. Satoshi Itoh, Kyushu University, JAPAN
Tech Info Division, Korea Atomic Energy, KOREA
Dr. R. England, Ciudad Universitaria, MEXICO
Bibliotheek, Fom-Inst Voor Plasma, NETHERLANDS
Prof. B.S. Liley, University of Waikato, NEW ZEALAND
Dr. Suresh C. Sharma, Univ of Calabar, NIGERIA
Prof. J.A.C. Cabral, Inst Superior Tech, PORTUGAL
Dr. Octavian Petrus, ALI CUZA University, ROMANIA
Prof. M.A. Hellberg, University of Natal, SO AFRICA
Dr. Johan de Villiers, Atomic Energy Bd, SO AFRICA
Fusion Div. Library, JEN, SPAIN
Prof. Hans Wilhelmson, Chalmers Univ Tech, SWEDEN
Dr. Lennart Stenflo, University of UMEA, SWEDEN
Library, Royal Inst Tech, SWEDEN
Dr. Erik T. Karlson, Uppsala Universitet, SWEDEN
Centre de Recherchesen, Ecole Polytech Fed, SWITZERLAND
Dr. W.L. Weise, Nat'l Bur Stand, USA
Dr. W.M. Stacey, Georg Inst Tech, USA
Dr. S.T. Wu, Univ Alabama, USA
Prof. Norman L. Oleson, Univ S Florida, USA
Dr. Benjamin Ma, Iowa State Univ, USA
Prof. Magne Kristiansen, Texas Tech Univ, USA
Dr. Raymond Askew, Auburn Univ, USA
Dr. V.T. Tolok, Kharkov Phys Tech Ins, USSR
Dr. D.D. Ryutov, Siberian Acad Sci, USSR
Dr. G.A. Eliseev, Kurchatov Institute, USSR
Dr. V.A. Glukhikh, Inst Electro-Physical, USSR
Institute Gen. Physics, USSR
Prof. T.J. Boyd, Univ College N Wales, WALES
Dr. K. Schindler, Ruhr Universitat, W. GERMANY
Nuclear Res Estab, Julich Ltd, W. GERMANY
Librarian, Max-Planck Institut, W. GERMANY
Dr. H.J. Kaeppler, University Stuttgart, W. GERMANY
Bibliothek, Inst Plasmaforschung, W. GERMANY